New Layered Uranium(VI) Molybdates: Syntheses and Structures of $(NH_3(CH_2)_3NH_3)(H_3O)_2(UO_2)_3(MoO_4)_5$, $C(NH_2)_3(UO_2)(OH)(MoO_4)$, $(C_4H_{12}N_2)(UO_2)(MoO_4)_2$, and $(C_5H_{14}N_2)(UO_2)(MoO_4)_2{\cdot}H_2O$

P. Shiv Halasyamani, Robin J. Francis,† Susan M. Walker, and Dermot O'Hare*

Inorganic Chemistry Laboratory, University of Oxford, South Parks Road, Oxford, UK OX1 3QR

Received July 17, 1998

Single crystals of $(NH_3(CH_2)_3NH_3)(H_3O)_2(UO_2)_3(MoO_4)_5$ (**1**), $C(NH_2)_3(UO_2)(OH)(MoO_4)$ (**2**), $(C_4H_{12}N_2)(UO_2)(MoO_4)_2$ (**3**) and $(C_5H_{14}N_2)(UO_2)(MoO_4)_2{\cdot}H_2O$ (**4**) have been synthesized hydrothermally by using $UO_2(CH_3COO)_2{\cdot}2H_2O$, $(NH_4)_2Mo_2O_7$, $HF_{(aq)}$, H_2O, and the respective organic template. The materials have layered structures with anionic uranium molybdate sheets separated by cationic organic templates. Compound **1** has an unprecedented uranium molybdate topology, whereas **2** is structurally related to johannite, $Cu[(UO_2)_2(SO_4)_2(OH)_2](H_2O)_8$, and **3** and **4** have layer topologies similar to zippiete, $K_2[UO_2(MoO_4)_2]$. Thermogravimetric measurements indicate all that four materials, after template loss, form a crystalline mixture of UO_2MoO_4 and MoO_3. Crystal data: $(NH_3(CH_2)_3NH_3)(H_3O)_2(UO_2)_3(MoO_4)_5$, orthorhombic, space group *Pbnm* (No. 62), with $a = 10.465(1)$ Å, $b = 16.395(1)$ Å, $c = 20.241(1)$ Å, and $Z = 4$; $C(NH_2)_3(UO_2)(OH)(MoO_4)$, monoclinic, space group $P2_1/c$ (No. 14), with $a = 15.411(1)$ Å, $b = 7.086(1)$ Å, $c = 18.108(1)$ Å, $\beta = 113.125(2)°$, and $Z = 4$; $(C_4H_{12}N_2)(UO_2)(MoO_4)_2$, triclinic, space group $P\bar{1}$ (No. 2), with $a = 7.096(1)$ Å, $b = 8.388(1)$ Å, $c = 11.634(1)$ Å, $\alpha = 97.008(3)°$, $\beta = 96.454(2)°$, $\gamma = 110.456(3)°$, and $Z = 2$; $(C_5H_{14}N_2)(UO_2)(MoO_4)_2{\cdot}H_2O$, orthorhombic, space group *Pbca* (No. 61), with $a = 12.697(1)$ Å, $b = 13.247(1)$ Å, $c = 17.793(1)$ Å, and $Z = 8$.

Introduction

Hydrothermal crystallization, in the presence of organic templating species, has been demonstrated to be a versatile technique for the synthesis of new materials with a variety of structural architectures.[1−8] By careful control of the synthesis conditions and the organic species employed, it has proven possible to synthesize a vast range of open framework and layered materials in which the cationic organic species is occluded within an anionic inorganic framework. Of paramount importance is the ability of the organic molecules to influence profoundly the structure of the synthesized product, and to direct their formation with particular structural and physical properties.[1,2] In aluminosilicate and metal phosphate chemistry, the ability of organic molecules to "template" the formation of particular structures is a well-established concept,[3−5] although the degree to which the final structures reflect the structural properties of the organic species varies greatly. The exact nature of the templating process is still open to much debate.[6] Nevertheless, the exquisite control over the detailed topology of the anionic framework that can be achieved by alteration of the steric and electronic properties of the template has been exploited to synthesize materials with an astonishingly diverse range of structural characteristics.

Aside from the purely academic interest in these fascinating reactions and structures, the range of materials chemistry applications for which these materials are suitable, such as heterogeneous catalysis,[7] molecular sieving, and ion-exchange,[8] has led to continued interest in the synthesis of new hybrid organic−inorganic layered and microporous materials. Although to date the vast majority of examples have been derived from main group elements such as silicon, aluminum, and phosphorus,[6,9,10] recently a wide variety of other main group and transition metals have been incorporated into three-dimensional and layered framework structures.[11−31] Such materials are of

† Current address: Department of Chemistry, University of Houston, 4800 Calhoun, Houston, Texas 77204-5641.

(1) Lok, B. M.; Cannon, T. R.; Messina, C. A. *Zeolites* **1983**, *3*, 282.
(2) Gies, H.; Marler, B. *Zeolites* **1992**, *12*, 42.
(3) Breck, D. W. *Zeolite Molecule Sieves: Structure, Chemistry and Use*; Wiley and Sons: London, 1974.
(4) Barrer, R. M. *Hydrothermal Chemistry of Zeolites*; Academic Press: London, 1982.
(5) Szostak, R. *Molecular Sieves: Principles of Synthesis and Identification*; Reinhold: New York, 1989.
(6) Davis, M. E.; Lobo, R. F. *Chem. Mater.* **1992**, *4*, 756.
(7) Venuto, P. B. *Microporous Mater.* **1994**, *2*, 297.
(8) Clearfield, A. *Chem. Rev.* **1988**, *88*, 125.
(9) Wilson, S. T.; Lok, B. M.; Messina, C. A.; Cannon, T. R.; Flanigen, E. M. *ACS Symp. Ser.* **1983**, *218*, 79.
(10) Flanigen, E. M.; Patton, R. L.; Wilson, S. T. *Stud. Surf. Sci. Catal.* **1988**, *37*, 13.
(11) Gier, T. E.; Stucky, G. D. *Nature* **1991**, *349*, 508.
(12) Loiseau, T.; Ferey, G. *J. Solid State Chem.* **1994**, *111*, 403.
(13) Loiseau, T.; Retoux, R.; Lacorre, P.; Ferey, G. *J. Solid State Chem.* **1994**, *111*, 427.
(14) Loiseau, T.; Ferey, G. *J. Mater. Chem.* **1996**, *6*, 1073.
(15) Ferey, G. *J. Fluor. Chem.* **1995**, *72*, 187.
(16) Chippindale, A. M.; Brech, S. J.; Cowley, A. R.; Simpson, W. M. *Chem. Mater.* **1996**, *8*, 2259.
(17) Haushalter, R. C.; Mundi, L. A. *Chem. Mater.* **1992**, *4*, 31.
(18) Khan, M. I.; Meyer, L. M.; Haushalter, R. C.; Schweitzer, A. L.; Zubieta, J.; Dye, J. L. *Chem. Mater.* **1996**, *8*, 43.
(19) Riou, D.; Ferey, G. *J. Solid State Chem.* **1994**, *111*, 422.
(20) Soghomonian, V.; Chen, Q.; Haushalter, R. C.; Zubieta, J.; O'Conner, C. J.; Lee, Y.-S. *Chem. Mater.* **1993**, *5*, 1690.
(21) Soghomonian, V.; Chen, Q.; Haushalter, R. C.; Zubieta, J. *Chem. Mater.* **1993**, *5*, 1595.
(22) Soghomonian, V.; Chen, Q.; Haushalter, R. C.; Zubieta, J. *Angew. Chem., Int. Ed. Engl.* **1993**, *32*, 610.
(23) Annen, M. J.; Davis, M. E.; Higgins, J. B.; Schlenker, J. L. *J. Chem. Soc., Chem. Commun.* **1991**, 1175.
(24) Gier, T. E.; Stucky, G. D. *Nature* **1991**, *349*, 508.

10.1021/ic980836r CCC: $18.00
Published on Web 12/31/1998

interest for two main reasons. First, the ability of some main group and transition metals to exist in five, six, seven, or higher coordination environments, as opposed to zeolites and aluminophosphates which only contain tetrahedrally coordinated units, allows for the synthesis of new and more complex framework architectures. Second, the incorporation of transition metals, which are capable of existing in a variety of different oxidation states within an open-framework structure, offers the possibility of combining the size and shape selectivity demonstrated by framework materials with the catalytic, magnetic, and photochemical properties associated with d-block elements. Metals that have been incorporated into layered and microporous frameworks through hydrothermal synthesis in the presence of organic templating agents include Be,[11] Ga,[12−14] In,[16] Mo,[32] V,[18−22] Zn,[23−26] Co,[27−30] and Fe.[31]

To date, with the exception of two uranium(VI) phosphates and a series of uranium(IV) fluorides that we recently reported,[33−35] we are not aware of any syntheses of hybrid organic−inorganic materials in which actinide elements such as uranium are incorporated into layered or microporous frameworks. We are interested in exploring the synthesis of actinide materials for a number of reasons. First, given the high coordination numbers and the variety of coordination geometries adopted by actinide elements, hydrothermal synthesis in the presence of bulky organic molecules could be expected to result in the formation of new, complex framework architectures. Clearfield and co-workers have demonstrated that in the synthesis of uranyl phosphonates, the presence of sterically demanding organic groups on the phosphonate ligands leads to the formation of novel structure types, including porous structures.[36−39] Second, actinide materials may be envisioned to exhibit useful catalytic, ion-exchange and intercalation properties. For example, hydrogen uranyl phosphate (HUP) is a fast hydrogen ion conductor and a versatile ion-exchange reagent.[40−43] Furthermore, Hutchings et al. recently demonstrated that uranium oxide based materials are effective oxidation catalysts for the destruction of a range of hydrocarbon and chlorine containing industrial pollutants.[44] Finally, the existence of a number of stable oxidation states in actinides, such as uranium, offers the possibility of synthesizing materials with useful magnetic properties. We have been exploring the synthesis of new uranium(VI) and uranium(IV) materials, with an aim toward not only synthesizing new and interesting materials, but also to synthesize these materials, in pure phase form, by varying intelligently the reagents and reagent concentrations. We report here the syntheses and structures of a new series of organically templated uranium(VI) molybdates, $(NH_3(CH_2)_3NH_3)(H_3O)_2$ $(UO_2)_3(MoO_4)_5$ (**1**), $C(NH_2)_3(UO_2)(OH)(MoO_4)$ (**2**), $(C_4H_{12}N_2)$ $(UO_2)(MoO_4)_2$ (**3**), and $(C_5H_{14}N_2)(UO_2)(MoO_4)_2 \cdot H_2O$ (**4**).

Experimental Section

Caution. Although all uranium materials used in these experiments were depleted, care should be taken in handling any uranium compounds.

Single crystals of **1** were synthesized initially by using U_3O_8 as the uranium precursor. Under all attempted reagent concentrations $(H_3O)Mo_3O_8(OH)_3$[45] was formed along with unreacted U_3O_8 and another unknown phase. Therefore the uranium precursor was changed to uranium acetate dihydrate, $UO_2(CH_3COO)_2 \cdot 2H_2O$. In doing so, the exclusive syntheses of **1**−**4** were accomplished.

Uranium acetate dihydrate, $UO_2(CH_3COO)_2 \cdot 2H_2O$, was synthesized by adding excess concentrated HNO_3 to 10 g of UO_2 (supplied by BNFL). This solution was stirred for 2 h, after which the acid was evaporated until a precipitate became visible, at which point the heat was removed and the solution was allowed to cool to room temperature. The yellow powder precipitate, $UO_2(NO_3)_2 \cdot 6H_2O$, was then heated to 380 °C, at 10 °C h^{-1}, held for 4 h, and cooled to room temperature at 5 °C h^{-1}. Once cooled, the orange-yellow solid produced was shown to be UO_3 by powder XRD. Excess glacial acetic acid and water were added to the UO_3 and the solution stirred for 2 h. The excess liquid was boiled off, and a resultant bright yellow powder was recovered in 90% yield. This powder was shown by elemental analysis to be phase pure. $UO_2(CH_3COO)_2 \cdot 2H_2O$ expt (calcd): C, 11.25 (11.33); H, 2.82 (2.38).

For $(NH_3(CH_2)_3NH_3)(H_3O)_2(UO_2)_3(MoO_4)_5$ (**1**): 1.16×10^{-1} g (2.9×10^{-4} mol) of $UO_2(CH_3COO)_2 \cdot 2H_2O$, 3.4×10^{-2} g (1×10^{-4} mol) of $(NH_4)_2Mo_2O_7$ (99%, Aldrich), 3.7×10^{-2} g (5×10^{-4} mol) of 1,3-diaminopropane (99%, Aldrich), 4.0×10^{-2} g (8×10^{-4} mol) of 40% $HF_{(aq)}$ (BDH), and 5.0 g (2.7×10^{-1} mol) of distilled H_2O were combined.

For $C(NH_2)_3(UO_2)(OH)(MoO_4)$ (**2**): 1.16×10^{-1} g (2.9×10^{-4} mol) of $UO_2(CH_3COO)_2 \cdot 2H_2O$, 1.7×10^{-1} g (5×10^{-4} mol) of $(NH_4)_2Mo_2O_7$, 3.7×10^{-2} g (5×10^{-4} mol) of guanidine hydrogen chloride (95%, Aldrich), 4.0×10^{-2} g (8×10^{-4} mol) of 40% $HF_{(aq)}$, and 5.0 g (2.7×10^{-1} mol) of distilled H_2O were combined.

For $(C_4H_{12}N_2)(UO_2)(MoO_4)_2$ (**3**): 1.16×10^{-1} g (2.9×10^{-4} mol) of $UO_2(CH_3COO)_2 \cdot 2H_2O$, 3.4×10^{-2} g (1×10^{-4} mol) of $(NH_4)_2Mo_2O_7$, 8.6×10^{-2} g (1.0×10^{-3} mol) of piperazine (99%, Aldrich), 4.0×10^{-2} g (8×10^{-4} mol) of 40% $HF_{(aq)}$, and 5.0 g (2.7×10^{-1} mol) of distilled H_2O were combined.

For $(C_5H_{14}N_2)(UO_2)(MoO_4)_2 \cdot H_2O$ (**4**): 1.16×10^{-1} g (2.9×10^{-4} mol) of $UO_2(CH_3COO)_2 \cdot 2H_2O$, 3.4×10^{-2} g (1×10^{-4} mol) of $(NH_4)_2Mo_2O_7$, 1.0×10^{-1} g (1.0×10^{-3} mol) of 2-methylpiperazine (99%, Aldrich), 4.0×10^{-2} g (8×10^{-4} mol) of 40% $HF_{(aq)}$, and 5.0 g (2.7×10^{-1} mol) of distilled H_2O were combined.

Each mixture was added to a separate Teflon pouch.[46] The pouches were sealed and placed in a 1 L autoclave filled with 300 mL of H_2O. The autoclave was heated at 180 °C for 24 h and cooled at 6 °C h^{-1} to room temperature. The pouches were opened and the respective products

(25) Harrison, W. T. A.; Broach, R. W.; Bedard, R. A.; Gier, T. E.; Bu, X.; Stucky, G. D. *Chem. Mater.* **1996**, *8*, 691.
(26) Harrison, W. T. A.; Phillips, M. L. F. *Chem. Mater.* **1997**, *9*, 1837.
(27) Chippindale, A. M.; Walton, R. I. *J. Chem. Soc., Chem. Commun.* **1994**, 2453.
(28) Chippindale, A. M.; Cowley, A. R. *Zeolites* **1997**, *18*, 176.
(29) Debord, J. R. D.; Haushalter, R. C.; Zubieta, J. *J. Solid State Chem.* **1996**, *125*, 270.
(30) Feng, P. Y.; Bu, X. H.; Stucky, G. D. *Nature* **1997**, *388*, 735.
(31) Debord, J. R. D.; Reiff, W. M.; Haushalter, R. C.; Zubieta, J. *J. Solid State Chem.* **1996**, *125*, 186.
(32) Haushalter, R. C.; Mundi, L. A. *Chem. Mater.* **1992**, *4*, 31.
(33) Francis, R. J.; Drewitt, M. J.; Halasyamani, P. S.; Ranganathachar, C.; O'Hare, D.; Clegg, W.; Teat, S. J. *Chem. Commun.* **1998**, 279.
(34) Francis, R. J.; Halasyamani, P. S.; O'Hare, D. *Angew. Chem., Int. Ed. Engl.* **1998**, *37*, 2214.
(35) Francis, R. J.; Halasyamani, P. S.; O'Hare, D. *Chem. Mater.* **1998**, *10*, 3131.
(36) Grohol, D.; Sumbamanian, M. A.; Poojary, D. M.; Clearfield, A. *Inorg. Chem.* **1996**, *35*, 5264.
(37) Poojary, D. M.; Grohol, D.; Clearfield, A. *Angew. Chem., Int. Ed. Engl.* **1995**, *34*, 1508.
(38) Poojary, D. M.; Grohol, D.; Clearfield, A. *J. Phys. Chem. Solids* **1995**, *56*, 1383.
(39) Poojary, D. M.; Cabeza, A.; Aranda, M. A. G.; Bruque, S.; Clearfield, A. *Inorg. Chem.* **1996**, *35*, 1468.
(40) Johnson, C. H.; Shilton, M. G.; Howe, A. T. *J. Solid State Chem.* **1981**, *37*, 37.
(41) Pozas-Tormo, R.; Moreno-Real, L.; Martinez-Lara, M.; Rodriguez-Castellon, E. *Can. J. Chem.* **1986**, *64*, 35.
(42) Moreno-Real, L.; Pozas-Tormo, R.; Martinez-Lara, M.; Bruque-Gamez, S. *Mater. Res. Bull.* **1987**, *22*, 19.
(43) Grohol, D.; Blinn, E. L. *Inorg. Chem.* **1997**, *36*, 3422.
(44) Hutchings, G. J.; Heneghan, C. S.; Hudson, I. D.; Taylor, S. H. *Nature* **1996**, *384*, 341.
(45) $(H_3O)Mo_3O_8(OH)_3$ was recovered as clear colorless needles. Single-crystal X-ray diffraction data were of poor quality ($R(F) \sim 20\%$), thus the stoichiometry should be taken as tentative.
(46) Harrison, W. T. A.; Nenoff, T. M.; Gier, T. E.; Stucky, G. D. *Inorg. Chem.* **1993**, *32*, 2437.

Table 1. Crystallographic Data for $(NH_3(CH_2)_3NH_3)(H_3O)_2(UO_2)_3(MoO_4)_5$ (**1**), $C(NH_2)_3(UO_2)(OH)(MoO_4)$ (**2**), $(C_4H_{12}N_2)(UO_2)(MoO_4)_2$ (**3**), and $(C_5H_{14}N_2)(UO_2)(MoO_4)_2 \cdot H_2O$ (**4**)

empirical formula	$U_3Mo_5O_{28}C_3H_{16}N_2$	$U_2Mo_2O_{16}C_{12}H_{14}N_2$	$UMo_2O_{10}C_4H_{12}N_2$	$UMo_2O_{12}C_5H_{16}N_2$
fw	1721.88	1016.1	678.05	710.07
space group	*Pbnm* (No.62)	$P2_1/c$ (No. 14)	$P\bar{1}$ (No. 2)	*Pbca* (No. 61)
a, Å	10.465(1)	15.411(1)	7.096(1)	12.697(1)
b, Å	16.395(1)	7.086(1)	8.388(1)	13.247(1)
c, Å	20.241(1)	18.108(1)	11.634(1)	17.793(1)
α, deg	90.0	90.0	97.008(3)	90.0
β, deg	90.0	113.125(2)	96.454(2)	90.0
γ, deg	90.0	90.0	110.456(3)	90.0
V, Å^3	3742.82(4)	1818.5(3)	634.9(3)	2992.7(3)
Z	4	4	2	8
ρ, g/cm^3	3.29	3.69	3.55	3.14
μ, cm^{-1}	157.7	191.8	147.1	125.0
$R(F)^a$	0.047	0.033	0.032	0.048
$R_w(F^2)^b$	0.134	0.077	0.092	0.118

[a] $R = \sum||F_o| - |F_c||/\sum|F_o|$. [b] $R_w = [\sum w(|F_o^2| - |F_c^2|)^2/\sum w(F_o^2)^2]^{1/2}$.

Table 2. Atomic Coordinates for $(NH_3(CH_2)_3NH_3)(H_3O)_2(UO_2)_3(MoO_4)_5$

atom	*x*	*y*	*z*	*U*(eq) (Å^2)[a]
U(1)	0.3766(1)	0.1905(1)	0.4327(1)	0.012(1)
U(2)	0.9466(1)	0.2701(1)	0.2500	0.012(1)
Mo(1)	0.6795(1)	0.2997(1)	0.3921(1)	0.012(1)
Mo(2)	0.3235(1)	0.1995(1)	0.2500	0.012(1)
Mo(3)	0.0246(1)	0.1848(1)	0.4238(1)	0.015(1)
O(1)	0.3082(8)	0.2834(6)	0.4051(4)	0.017(2)
O(2)	0.4420(7)	0.0962(6)	0.4603(4)	0.017(2)
O(3)	0.5787(8)	0.2123(6)	0.3807(4)	0.018(2)
O(4)	0.3661(7)	0.1435(6)	0.3225(4)	0.015(2)
O(5)	0.1722(7)	0.1297(6)	0.4217(4)	0.016(2)
O(6)	0.2831(8)	0.2081(7)	0.5387(4)	0.021(2)
O(7)	0.5165(8)	0.2685(7)	0.4979(5)	0.025(2)
O(8)	0.0192(8)	0.2590(6)	0.3600(4)	0.018(2)
O(9)	−0.0965(9)	0.1152(8)	0.4127(5)	0.032(2)
O(10)	0.5923(9)	0.3886(7)	0.3968(5)	0.024(2)
O(11)	0.7781(7)	0.3070(6)	0.3211(4)	0.014(2)
O(12)	0.4023(13)	0.2918(10)	0.2500	0.024(3)
O(13)	0.1561(13)	0.2150(11)	0.2500	0.027(3)
O(14)	0.8915(11)	0.1674(9)	0.2500	0.018(3)
O(15)	1.0041(11)	0.3726(9)	0.2500	0.019(3)
C(1)	0.6359(17)	0.0482(16)	0.2500	0.028(5)
C(2)	0.7072(13)	0.0178(10)	0.3108(7)	0.025(3)
O(16)	0.0772(16)	0.4264(11)	0.3972(9)	0.078(6)
N(1)	0.6340(13)	0.0383(9)	0.3722(7)	0.037(3)

[a] *U*(eq) is defined as one-third of the trace of the orthogonalized $\mathbf{U}_{ij}$ tensor.

Table 3. Selected Bond Distances (Å) for $(NH_3(CH_2)_3NH_3)(H_3O)_2(UO_2)_3(MoO_4)_5$[a]

U(1)−O(1)	1.773(10)
U(1)−O(2)	1.780(9)
U(1)−O(3)	2.391(8)
U(1)−O(4)	2.363(8)
U(1)−O(5)	2.370(8)
U(1)−O(6)	2.374(8)
U(1)−O(7)	2.349(8)
U(2)−O(8)#2	2.359(8)
U(2)−O(8) #3	2.359(8)
U(2)−O(11) #1	2.356(8)
U(2)−O(11)	2.356(8)
U(2)−O(13) #2	2.371(13)
U(2)−O(14)	1.780(14)
U(2)−O(15)	1.785(14)
Mo(1)−O(3)	1.794(10)
Mo(1)−O(6) #4	1.777(8)
Mo(1)−O(10)	1.722(10)
Mo(1)−O(11)	1.772(8)
Mo(2)−O(4)	1.788(9)
Mo(2)−O(4) #1	1.788(9)
Mo(2)−O(12)	1.72(2)
Mo(2)−O(13)	1.770(13)
Mo(3)−O(5)	1.789(9)
Mo(3)−O(7) #5	1.762(9)
Mo(3)−O(8)	1.776(10)
Mo(3)−O(9)	1.719(11)

[a] Symmetry transformations used to generate equivalent atoms: #1, $x, y, -z + 1/2$; #2, $x + 1, y, z$; #3, $x + 1, y, -z + 1/2$; #4, $x + 1/2, -y + 1/2, -z + 1$; #5 $x - 1/2, -y + 1/2, -z + 1$.

recovered by filtration and washed with distilled H_2O and acetone. In all instances pure phase products were formed as clear yellow crystals in 45%, 25%, 45%, and 40% yields based on uranium for **1**, **2**, **3**, and **4**, respectively.

Crystallographic Determination. All crystallographic data were acquired using graphite monochromated Mo Kα ($\lambda = 0.710\,73$ Å) radiation on an Enraf-Nonius DIP 2000 image-plate diffractometer with a step of 2° per frame, $\theta_{max} = 26°$. The crystals were mounted on a glass fiber under paratone oil and cooled to 150.0(2) K on the diffractometer. Each frame was collected, indexed, and processed using DENZO,[47] and the files scaled together using SCALEPACK.[47] For all of the structures the heavy atoms positions were determined using SIR92[48] and refined using SHELXL-93.[49] All non-hydrogen atoms were refined with anisotropic thermal parameters, except for **3** in which the occluded water and template molecule were refined isotropically, using full-matrix least-squares procedures on F_o^2 with $I > 2\sigma(I)$. Hydrogen atoms were fixed in geometrically idealized positions and allowed to ride on their attached carbon, nitrogen, or oxygen atom with isotropic thermal parameters according to the atom to which they were connected (these were not refined). The assignment of the nitrogen atom on the piperazine and 2-methylpiperazine ring was inferred from hydrogen bonding interactions with the uranium molybdate layer. An empirical data correction using XABS2[50] was applied. All calculations were performed using the WinGX-98[51] crystallographic software package. Selected crystallographic data for each compound are given in Table 1. Fractional atomic coordinates, thermal parameters, and pertinent bond lengths are listed in Tables 2−9.

Ion-Exchange Experiments. Ion-exchange reactions were attempted by stirring ca. 100 mg of product in 10 mL of 1 M aqueous solution of the following metal salts, $NaNO_3$, KNO_3, $Co(CH_3CO_2)_2 \cdot 4H_2O$, $CuCl_2 \cdot 2H_2O$, $FeCl_2 \cdot 4H_2O$, $Mn(CH_3CO_3)_2 \cdot 4H_2O$, $NiCl_2 \cdot 6H_2O$. The

(47) Otwinowski, Z. *Data Collection and Processing, Proceedings of the CCP4 study weekend*; Otwinowski, Z., Ed.; Daresbury Laboratory: Warrington, U.K., 1993.
(48) Altomare, A.; Cascarano, G.; Giacovazzo, C.; Guagliardi, A.; Polidor, G.; Burla, M. C.; Camalli, M. *J. Appl. Crystallogr.* **1994**, *27*, 435.
(49) Sheldrick, G. M. *SHELXL-93: A program for crystal structure refinement*; Sheldrick, G. M., Ed.; University of Gottingen: Germany, 1993.
(50) Parkin, S.; Moezzi, B.; Hope, H. *J. Appl. Crystallogr.* **1995**, *28*, 53.
(51) Farrugia, L. J. *WinGX: An integrated system of publically available windows programs for the solution, refinement, and analysis of single-crystal X-ray diffraction data.*; Farrugia, L. J., Ed.; University of Glasgow: Scotland, 1998.

Table 4. Atomic Coordinates and Thermal Parameters for $C(NH_2)_3(UO_2)(OH)(MoO_4)$

atom	*x*	*y*	*z*	*U*(eq) (Å^2)[a]
U(1)	0.1408(1)	0.0460(1)	0.3990(1)	0.010(1)
U(2)	0.3369(1)	0.0029(1)	0.6179(1)	0.010(1)
Mo(1)	0.4130(1)	0.5178(1)	0.7124(1)	0.011(1)
Mo(2)	0.0826(1)	−0.4743(1)	0.3035(1)	0.010(1)
O(1)	0.4178(4)	0.0501(9)	0.5719(4)	0.020(1)
O(2)	0.3791(4)	0.5999(9)	0.7853(3)	0.020(1)
O(3)	0.2396(4)	−0.1525(8)	0.5018(3)	0.014(1)
O(4)	0.2271(4)	0.1965(7)	0.5206(3)	0.010(1)
O(5)	0.3551(4)	0.3021(8)	0.6745(3)	0.014(1)
O(6)	0.0490(4)	−0.0051(7)	0.4321(3)	0.010(1)
O(7)	0.2357(4)	0.1040(8)	0.3693(3)	0.016(1)
O(8)	0.1331(4)	−0.2559(8)	0.3461(3)	0.020(1)
O(9)	0.0371(4)	−0.4346(9)	0.2366(3)	0.017(1)
O(10)	0.0909(4)	−0.6364(8)	0.3818(3)	0.015(1)
O(11)	0.1441(4)	−0.5656(9)	0.2506(4)	0.019(1)
O(12)	0.3821(4)	0.6841(8)	0.6319(3)	0.018(1)
O(13)	0.2539(4)	−0.0536(8)	0.6604(3)	0.016(1)
O(14)	0.5375(4)	0.4792(8)	0.7550(3)	0.017(1)
C(1)	0.3697(7)	0.5549(16)	0.4242(6)	0.028(2)
C(2)	0.1287(6)	0.4856(13)	0.6094(5)	0.019(2)
N(1)	0.3389(6)	0.4795(11)	0.4767(5)	0.029(2)
N(2)	0.3633(7)	0.4595(16)	0.3598(6)	0.043(3)
N(3)	0.4073(7)	0.7270(13)	0.4371(6)	0.039(2)
N(4)	0.1223(6)	−0.4394(12)	0.5397(4)	0.024(2)
N(5)	0.1624(6)	0.5842(12)	0.6766(4)	0.026(2)
N(6)	0.0963(5)	0.3118(11)	0.6103(4)	0.023(2)

[a] U(eq) is defined as one-third of the trace of the orthogonalized $\mathbf{U}_{ij}$ tensor.

Table 5. Selected Bond Distances (Å) for $C(NH_2)_3(UO_2)(OH)(MoO_4)$[a]

U(1)−O(3)	2.353(5)
U(1)−O(4)	2.335(5)
U(1)−O(6)	1.777(6)
U(1)−O(7)	1.793(6)
U(1)−O(8)	2.328(6)
U(1)−O(9) #1	2.349(5)
U(1)−O(10) #2	2.359(6)
U(2)−O(13)	1.778(6)
U(2)−O(1)	1.782(6)
U(2)−O(3)	2.325(5)
U(2)−O(4)	2.347(5)
U(2)−O(5)	2.323(5)
U(2)−O(12) #3	2.348(6)
U(2)−O(14) #4	2.360(5)
Mo(1)−O(2)	1.702(6)
Mo(1)−O(5)	1.767(5)
Mo(1)−O(12)	1.787(6)
Mo(1)−O(14)	1.786(6)
Mo(2)−O(8)	1.767(6)
Mo(2)−O(9)	1.788(5)
Mo(2)−O(10)	1.790(6)
Mo(2)−O(11)	1.717(6)

[a] Symmetry transformations used to generate equivalent atoms: #1, $-x, y + {}^1/_2, -z + {}^1/_2$; #2, $x, y + 1, z$; #3, $x, y - 1, z$; #4, $-x + 1, y - {}^1/_2, -z + {}^3/_2$.

reactions were performed at room temperature and 60 °C for 24 h. Although products from the reaction were shown, by elemental analysis, to contain a few percent of the exchanged metal, C, H, and N were also found. In no instance was complete exchange observed.

Infrared and Raman Spectroscopy. FTIR spectra were collected on a Perkin-Elmer FT 1710 spectrometer using Nujol mulls of samples pressed between KBr plates. Raman spectra were collected using a Dilor Labram laser spectrometer on crystals mounted on microscope slides.

Thermogravimetric Analysis. TGA measurements were performed on a Rheometric Scientific STA 1500H thermal analyzer. The samples were contained within platinum crucibles and heated at a rate of 5 °C min^{-1} from room temperature to 500 °C in static air.

Table 6. Atomic Coordinates and Thermal Parameters for $(C_4H_{12}N_2)(UO_2)(MoO_4)_2$

atom	*x*	*y*	*z*	*U*(eq) (Å^2)[a]
U(1)	0.2930(1)	0.0281(1)	0.2414(1)	0.004(1)
Mo(1)	0.7869(1)	0.0917(1)	0.1041(1)	0.004(1)
Mo(2)	0.3722(1)	0.1513(1)	0.5682(1)	0.005(1)
O(1)	0.7975(7)	−0.0034(6)	−0.0377(4)	0.010(1)
O(2)	0.2042(6)	0.0713(6)	0.4292(4)	0.009(1)
O(3)	0.2449(7)	0.2260(6)	0.6704(4)	0.011(1)
O(4)	0.1561(7)	−0.1987(6)	0.2289(4)	0.010(1)
O(5)	0.9902(7)	0.0853(6)	0.2054(4)	0.012(1)
O(6)	0.5532(6)	0.0151(5)	0.3817(4)	0.009(1)
O(7)	0.5497(6)	−0.0281(5)	0.1441(4)	0.008(1)
O(8)	0.5857(7)	0.3264(6)	0.5591(4)	0.013(1)
O(9)	0.4341(7)	0.2537(6)	0.2511(4)	0.009(1)
O(10)	0.8076(7)	0.3048(6)	0.1068(4)	0.015(1)
N(1)	0.9682(8)	0.3464(7)	0.5495(5)	0.009(1)
N(2)	0.6113(9)	0.5476(8)	0.1176(5)	0.014(1)
C(1)	1.0082(11)	0.3496(8)	0.4268(6)	0.011(1)
C(2)	0.9296(11)	0.4775(9)	0.3751(6)	0.013(1)
C(3)	0.7175(11)	0.5983(9)	0.0171(6)	0.016(1)
C(4)	0.3929(12)	0.5300(10)	0.0941(6)	0.016(2)

[a] *U*(eq) is defined as one-third of the trace of the orthogonalized $\mathbf{U}_{ij}$ tensor.

Table 7. Selected Bond Distances (Å) for $(C_4H_{12}N_2)(UO_2)(MoO_4)_2$[a]

U(1)−O(1) #1	2.350(4)
U(1)−O(2)	2.361(4)
U(1)−O(4)	1.787(5)
U(1)−O(5) #2	2.364(4)
U(1)−O(6)	2.365(4)
U(1)−O(7)	2.400(4)
U(1)−O(9)	1.787(4)
Mo(1)−O(1)	1.764(4)
Mo(1)−O(5)	1.779(4)
Mo(1)−O(7)	1.779(4)
Mo(1)−O(10)	1.737(5)
Mo(2)−O(2)	1.797(4)
Mo(2)−O(3)	1.754(5)
Mo(2)−O(6) #3	1.793(4)
Mo(2)−O(8)	1.727(5)

[a] Symmetry transformations used to generate equivalent atoms: #1, $-x + 1, -y, -z$; #2, $x - 1, y, z$; #3, $-x + 1, -y, -z + 1$.

Results

Compound (**1**) contains a layer topology, shown in Figure 1, that is unprecedented with respect to U^{VI} materials. The layers are constructed from uranium pentagonal bipyramids corner linked to molybdenum tetrahedra. Each uranium pentagonal bipyramid is surrounded by five molybdenum tetrahedra, whereas each molybdenum tetrahedron is connected to three uranium polyhedra. The alternation of the tetrahedra and pentagonal bipyramids produce hexagonal "holes" within the layer. Thus in connectivity terms, each layer can be described as $\{3[UO_{2/1}O_{5/2}]^{3-}\ 5[MoO_{3/2}O_{1/1}]\}^{4-}$ (see Figure 1). These anionic layers are separated by the cationic template molecule, 1,3-diaminopropane, and hydronium cation. Hydrogen bonding interactions, N−H···O and O−H···O, are observed between the template and the anionic layer as well as the template and the hydronium molecule. Bond valence calculations[52,53] on **1** resulted in values ranging from 5.70 to 5.96 for Mo^{VI}, with oxygen valences ranging from 1.55 to 2.31. Bond valence parameters for uranium were taken from Burns et al.,[54] which resulted in values of 6.03 and 6.04 for U^{VI}. The two crystallo-

(52) Brown, I. D.; Altermatt, D. *Acta Crystallogr.* **1985**, *B41*, 244.
(53) Brese, N. E.; O'Keefe, M. *Acta Crystallogr.* **1991**, *B47*, 192.
(54) Burns, P. C.; Ewing, R. C.; Hawthorne, F. C. *Can. Miner.* **1997**, *35*, 1551.

Table 8. Atomic Coordinates and Thermal Parameters for $(C_5H_{14}N_2)(UO_2)(MoO_4)_2 \cdot H_2O$

atom	*x*	*y*	*z*	*U*(eq) (Å^2)[a]
U(1)	0.1465(1)	0.2095(1)	0.5231(1)	0.007(1)
Mo(1)	0.1209(1)	−0.0860(1)	0.5292(1)	0.008(1)
Mo(2)	0.0955(1)	0.6308(1)	0.4224(1)	0.009(1)
O(1)	0.3211(5)	0.1555(5)	0.5027(4)	0.008(1)
O(2)	−0.0344(6)	0.1575(5)	0.5298(4)	0.012(2)
O(3)	0.0391(6)	0.3454(5)	0.5589(5)	0.015(2)
O(4)	0.1271(6)	0.2415(6)	0.4274(5)	0.017(2)
O(5)	0.1668(6)	0.1767(6)	0.6193(4)	0.014(2)
O(6)	0.1379(6)	0.0361(6)	0.4901(5)	0.016(2)
O(7)	0.2437(6)	−0.1485(6)	0.5358(5)	0.016(2)
O(8)	0.0692(7)	−0.0736(6)	0.6182(5)	0.022(2)
O(9)	0.1025(6)	0.5041(6)	0.3983(5)	0.021(2)
O(10)	0.1359(7)	0.7006(7)	0.3472(5)	0.025(2)
O(11)	0.2550(7)	0.8824(6)	0.3308(6)	0.026(2)
N(1)	−0.0651(8)	0.0422(8)	0.7094(6)	0.023(2)*
N(2)	−0.0799(8)	0.3988(7)	0.3637(6)	0.019(2)*
C(1)	−0.0616(10)	0.3206(9)	0.3050(7)	0.021(2)*
C(2)	−0.0055(11)	0.1295(10)	0.7391(8)	0.028(3)*
C(3)	−0.0902(10)	−0.0345(9)	0.7682(7)	0.021(2)*
C(4)	0.1434(9)	0.5172(8)	0.6647(6)	0.016(2)*
C(5)	−0.1578(11)	−0.1151(11)	0.7372(8)	0.031(3)*

[a] *U*(eq) is defined as one-third of the trace of the orthogonalized $\mathbf{U}_{ij}$ tensor. Atoms marked with asterisks were refined isotropically.

Table 9. Selected Bond Distances (Å) for $(C_5H_{14}N_2)(UO_2)(MoO_4)_2 \cdot H_2O$[a]

U(1)−O(1)	2.357(7)
U(1)−O(2)	2.402(7)
U(1)−O(3)	2.346(7)
U(1)−O(4)	1.773(8)
U(1)−O(5)	1.783(8)
U(1)−O(6)	2.373(8)
U(1)−O(7) #1	2.352(7)
Mo(1)−O(2) #2	1.790(7)
Mo(1)−O(6)	1.774(8)
Mo(1)−O(7)	1.769(8)
Mo(1)−O(8)	1.721(9)
Mo(2)−O(1) #1	1.810(7)
Mo(2)−O(3) #3	1.770(7)
Mo(2)−O(9)	1.735(8)
Mo(2)−O(10)	1.704(9)

[a] Symmetry transformations used to generate equivalent atoms: #1, $-x + {}^1/_2, y + {}^1/_2, z$; #2, $-x, -y, -z + 1$; #3 $-x, -y + 1, -z + 1$.

graphically unique U^{VI} cations contain nearly linear uranyl units, with U═O distances ranging from 1.773(10) to 1.785(14) Å. The remaining five oxygens are equatorially coordinated with U−O distances ranging from 2.349(8) to 2.374(8) Å. The U−O bond distances are in very good agreement with the average values determined by Burns *et al.*[54] for pentagonal bipyramidal uranium, which are 1.79(4) for a uranyl bond and 2.37(9) for a U−O equatorial bond. Each Mo^{VI} is tetrahedrally coordinated to four oxygens. Three of the four oxygens bridge to a uranium cation, whereas the fourth remains terminal. The bridging Mo−O distances range from 1.762(9) to 1.794(9) Å, with Mo−O terminal distances ranging from 1.719(11) to 1.722(10) Å.

Compound **2** contains a layer topology is similar to the naturally occurring mineral johannite,[55] $Cu[(UO_2)_2(SO_4)_2(OH)_2](H_2O)_8$ (see Figure 2). Unlike **1**, the uranium polyhedra share edges and form dimers that are surrounded by six molybdenum tetrahedra (see Figure 3). This alternation of the uranium polyhedra and molybdenum tetrahedra produces hexagonal "holes" in the layer. In connectivity terms the layer can be described as $\{[UO_{2/1}O_{3/2}(OH)_{2/2}]^{2-}[MoO_{1/1}O_{3/2}]^{+}\}^{-}$. Bond valence calculations on **2** resulted in values of 5.86 and 5.88 for Mo^{VI} and 6.11 and 6.16 for U^{VI}. Except for the oxygens bridging the uranium atoms, oxygen valences ranged from 1.67 to 2.27. Protonation of O(2) and O(4), the oxygen atoms that bridge the uranium atoms, was inferred from bond valence calculations that resulted in values of 0.97 and 0.96, respectively. Similar to **1**, the two unique U^{VI} in **2** are in seven-coordinate pentagonal bipyramidal geometries, with nearly linear uranyl bonds, and short U═O distances ranging from 1.776(6) to 1.793(6) Å. The molybdenum tetrahedra are coordinated to four oxygens, three

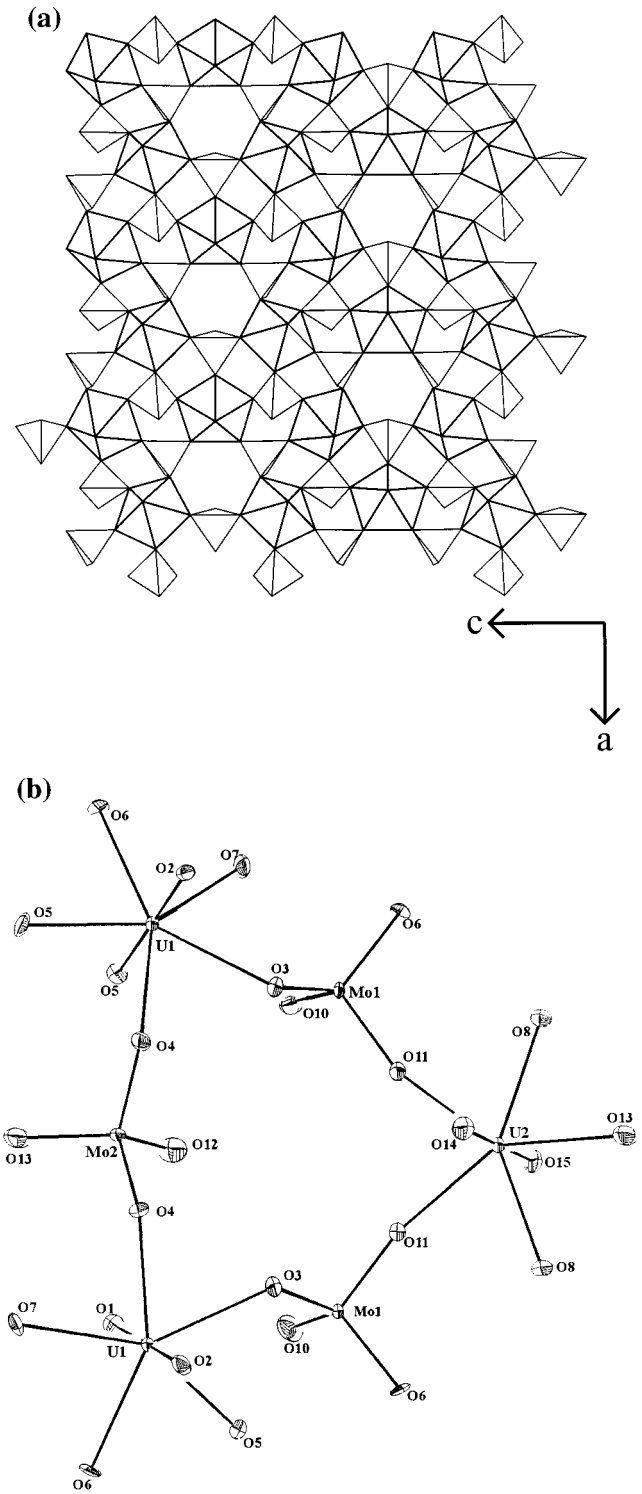

Figure 1. (a) Polyhedral representation of the uranium molybdate layer in $(NH_3(CH_2)_3NH_3)(H_3O)_2(UO_2)_3(MoO_4)_5$ and (b) ORTEP (50% probability ellipsoids) of the uranium molybdate unit.

(55) Mereite, K. *Tschermaks Mineral. Petrogr. Mitt.* **1982**, *30*, 49.

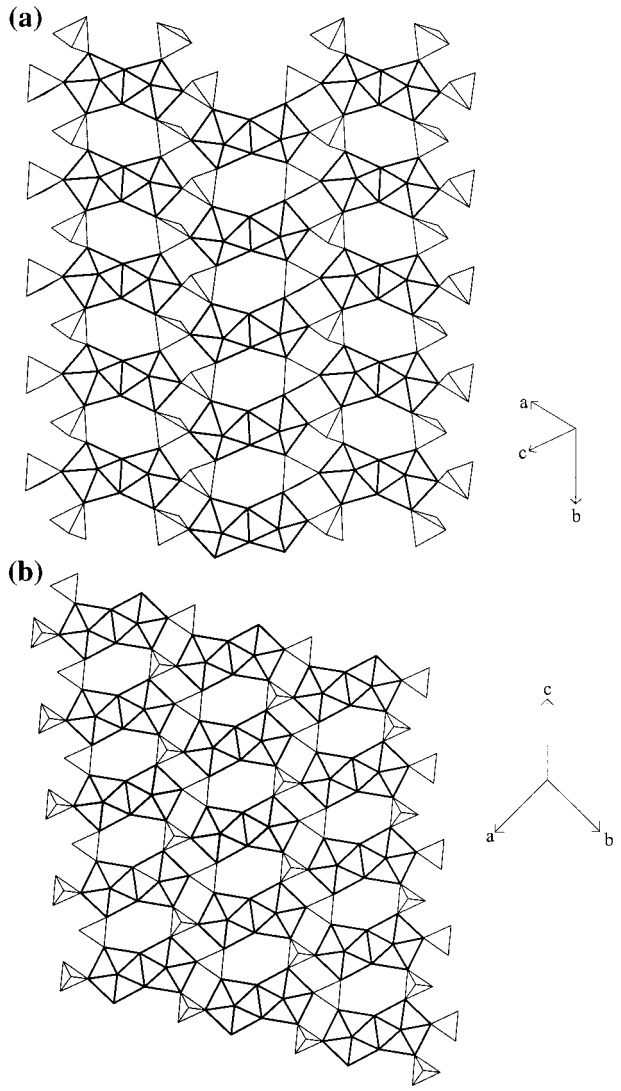

Figure 2. Polyhedral representation of the uranium molybdate layer in (a) $C(NH_2)_3(UO_2)(OH)(MoO_4)$ and (b) johannite, $Cu[(UO_2)_2(SO_4)_2(OH)_2](H_2O)_8$.

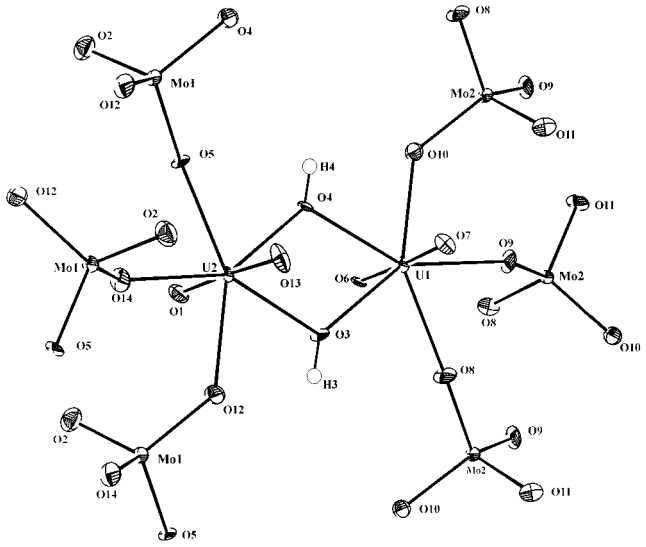

Figure 3. ORTEP representation (50% probability ellipsoids) of the uranium molybdate unit in $C(NH_2)_3(UO_2)(OH)(MoO_4)$.

of which bridge to a uranium and the fourth remains terminal. The terminal distances, 1.702(5) and 1.717(6) Å, are shorter

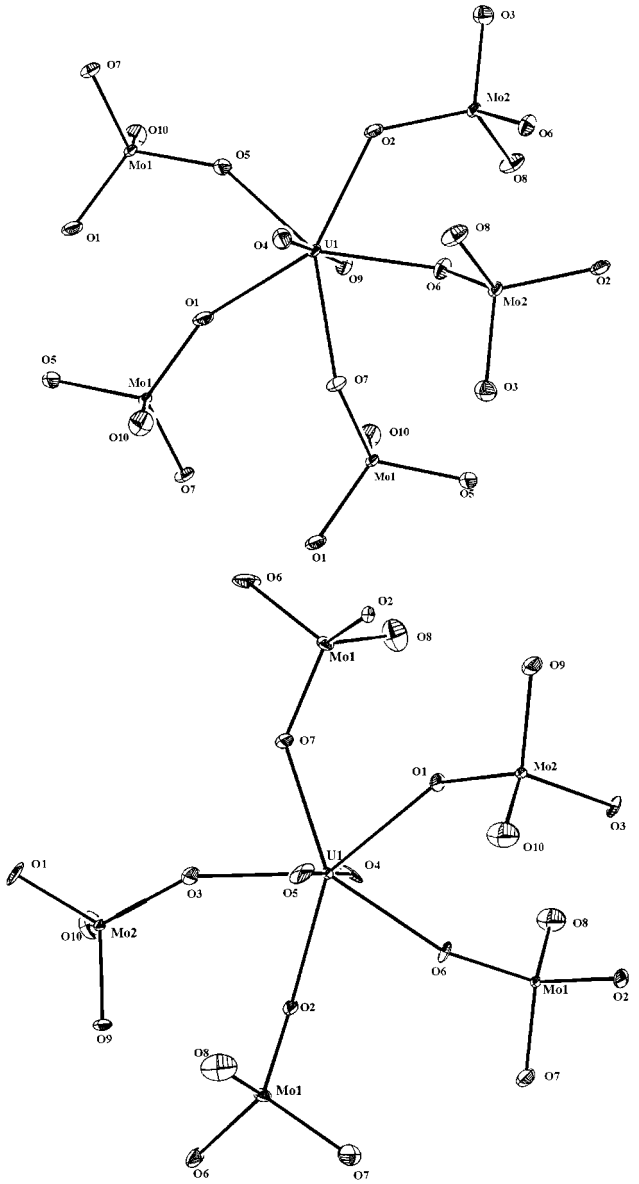

Figure 4. ORTEP representation (50% probability ellipsoids) of the uranium molybdate unit in $(C_4H_{12}N_2)(UO_2)(MoO_4)_2$ (top) and $(C_5H_{14}N_2)(UO_2)(MoO_4)_2{\cdot}H_2O$ (bottom).

than the bridging Mo−O distances that range from 1.767(5) to 1.790(5) Å. These anionic layers are separated by cationic guanidinium template molecules.

Compounds **3** and **4** have uranium molybdenum topologies that are similar to zippiete, $K_2[UO_2(MoO_4)_2]$.[56] With both **3** and **4** the uranium polyhedra are corner linked to five molybdenum tetrahedra (see Figure 4a and b). In connectivity terms, for both **3** and **4** the layers can be described as $\{[UO_{2/1}O_{5/2}]^{3-}2[MoO_{3/2}O_{1/1}]^{+}\}^{-}$. Bond valence calculations on **3** and **4** resulted in values ranging from 5.71 to 5.88 for the Mo^{VI} cation, and 5.97 and 6.04 for U^{VI}, with oxygen valences ranging from 1.49 to 2.02. As with **1** and **2**, the uranium cations in **3** and **4** are in seven-coordinate pentagonal bipyramidal geometries, with nearly linear uranyl units, and short U═O bonds of 1.787(5) Å. Both **3** and **4** have two crystallographically unique Mo^{VI}, both of which are linked to three bridging and one terminal oxygen, with bond distances for the bridging oxygen ranging from

(56) Sadikov, G. G.; Krasovskaya, T. I.; Polyakov, Y. A.; Nikolaev, V. P. *Inorg. Mater.* **1988**, *24*, 91.

Table 10. Infrared and Raman Vibrations

	IR (cm^{-1})			Raman (cm^{-1})		
	Mo−O	U−O	U−O−Mo	Mo−O	U−O	U−O−Mo
$(NH_3(CH_2)_3NH_3)(H_3O)_2(UO_2)_3(MoO_4)_5$	901	787	722	938	816	760
			652			
			528			
$C(NH_2)_3(UO_2)(OH)(MoO_4)$	900	787		950	813	774
				1000		754
$(C_4H_{12}N_2)(UO_2)(MoO_4)_2$	915	787	759	928		807
	877		722	915		798
			668	900		776
			576			762
$(C_5H_{14}N_2)(UO_2)(MoO_4)_2 \cdot H_2O$	901	780	723	928	812	723

Table 11. Hydrogen Bonding Interactions of $(NH_3(CH_2)_3NH_3)(H_3O)_2(UO_2)_3(MoO_4)_5$ (**1**), $C(NH_2)_3(UO_2)(OH)(MoO_4)$ (**2**), $(C_4H_{12}N_2)(UO_2)(MoO_4)_2$ (**3**), and $(C_5H_{14}N_2)(UO_2)(MoO_4)_2 \cdot H_2O$ (**4**)

	D···A (Å)	
$(NH_3(CH_2)_3NH_3)(H_3O)_2(UO_2)_3(MoO_4)_5$	N(1)···O(2)	2.851(4)
	N(1)···O(3)	2.916(4)
	N(1)···O(16)	2.917(5)
$C(NH_2)_3(UO_2)(OH)(MoO_4)$	N(1)···O(4)	2.945(6)
	N(1)···O(12)	2.995(5)
	N(3)···O(2)	2.883(5)
	N(3)···O(6)	2.996(6)
	N(4)···O(3)	2.975(6)
	N(5)···O(13)	2.998(5)
	N(6)···O(11)	2.928(6)
$(C_4H_{12}N_2)(UO_2)(MoO_4)_2$	N(1)···O(3)	2.811(4)
	N(1)···O(8)	2.683(4)
	N(2)···O(3)	2.772(4)
	N(2)···O(10)	2.844(4)
$(C_5H_{14}N_2)(UO_2)(MoO_4)_2 \cdot H_2O$	N(1)···O(8)	2.811(13)
	N(1)···O(11)	2.703(14)
	N(2)···O(1)	2.783(13)
	N(2)···O(9)	2.771(13)

1.739(8) to 1.810(7) Å and terminal Mo−O distances ranging from 1.704(9) to 1.737(5) Å. The anionic uranium−molybdate layers in **3** and **4** are separated by piperazinium or 2-methylpiperazinium molecules, respectively. Both of these templates are inferred to be doubly protonated and interact with the anion layer through N−H···O hydrogen bonding.

Infrared and Raman Spectroscopy. The bands and assignments for the IR and Raman spectra for **1**, **2**, **3**, and **4** are listed in Table 10. Mo−O vibrations are observed in both the IR and Raman and occur between 890 and 1000 cm^{-1}. The $\nu(UO_2)^{2+}$ symmetric vibration is also observed in both the IR and Raman and is found between 780 and 850 cm^{-1}. Multiple bands, occurring between 500 and 800 cm^{-1}, are also observed and are attributable to U-O−Mo asymmetric and symmetric vibrations. All four materials have a broad vibration centered at 3400 cm^{-1} owing to the template vibrations, whereas **1**, **2**, and **3** also have a band at 1610 cm^{-1} attributable to a water bending mode. The above assignments are consistent with those reported previously for uranium and molybdenum oxides.[57]

Thermogravimetric Measurements. Thermogravimetric measurements on **1**−**4** revealed similar behavior in each case. For **1** and **4**, the materials with occluded water (or hydronium), an initial weight loss of 2−5% between room temperature and 150 °C was observed and can be attributed to the loss of water. A second weight loss of 5−10% occurs between 250 and 350 °C and is due to the loss of the template molecule. For materials **2** and **4**, the first weight loss event occurs between 200 and 300 °C and is attributable to the loss of template. Elemental analysis on the calcined materials confirmed the loss of template as no C, H, or N was detected. In addition, powder XRD measurements on the calcined materials revealed that the compounds converted to a mixture of crystalline UO_2MoO_{58} and MoO_3 (see Supporting Information).

Discussion

Compounds **1**−**4** represent the first examples of organically templated uranium molybdate phases. All four materials contain metal cations in similar coordination environments. Each U^{VI} cation is found in a seven coordinate pentagonal bipyramidal geometry, whereas each molybdenum cation is found in a tetrahedral coordination. However, because of the different connectivity of the polyhedra distinct layer topologies are observed. The uranium molybdate layer in **1** is unprecedented, whereas the topology in **2** is similar to the mineral johannite, and **3** and **4** are related to zippiete. Although, in general, the complexity of hydrothermal crystallizations precludes a complete understanding of the factors promoting the formation of a particular layer structure, a discussion of possible reasons for the occurrence of each layer topology seems relevant.

As with many organically templated organic−inorganic phases, one major factor that seems to control the nature of the layer topology formed is the establishment of favorable hydrogen and ionic bonding interactions between the organic template and the inorganic framework. This is amply illustrated in compound **1** (see Figure 1). The layer structure of **1** is shown in Figure 1. Each uranium polyhedron is surrounded by five molybdenum tetrahedra via bridging oxygens. The alternation of U^{VI} and Mo^{VI} polyhedra is such that roughly hexagonal "holes" are generated within the layers. The 1,3-diaminopropane template molecule spans these holes such that N−H···O hydrogen bonding interactions between the template, uranyl oxygens and bridging oxygens are maximized (see Figure 5a). Additional N−H···O hydrogen bonds between the template and the occluded water molecules create a complex network of hydrogen bonding interactions and further bind the structure together (see Table 11). The observation that the template spans the "hole" suggested that the use of longer chain amine templates may produce larger holes and confer on these materials genuine microporosity. However, thus far reactions employing 1,4-diaminobutane and 1,6-diaminohexane as templates have failed to produce phase pure products or crystals suitable for single-crystal X-ray structure determination, although attempts are ongoing.

Compound **2**, which contains a layer topology very similar to the mineral johannite,[55] also contains a strong network of hydrogen bonding interactions. The layer structure of **2** is shown in Figure 2 and contains dimeric units formed from edge sharing uranium bipyramids linked to six molybdenum tetrahedra

(57) Adams, D. M. *Metal−Ligand and Related Vibrations*; Edward Arnold: London, 1967.

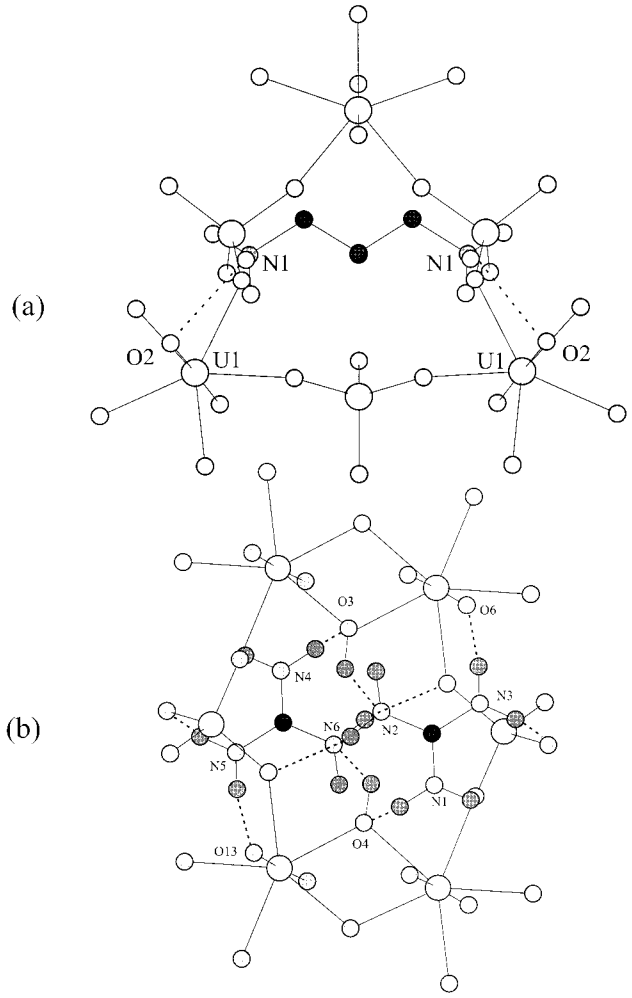

Figure 5. Hydrogen bonding interactions between the organic template in (a) $(NH_3(CH_2)_3NH_3)(H_3O)_2(UO_2)_3(MoO_4)_5$ and (b) $C(NH_2)_3(UO_2)(OH)(MoO_4)$.

through corner sharing oxygen atoms. It has been suggested[59] that it is energetically unfavorable for a $M^{VI}O_4$ tetrahedra to share an edge with a UO_7 pentagonal bipyramid. A consequence of the fully corner shared topology is that a roughly hexagonal "hole" is created within the layer. It is found that the guanidinium cation resides between the layers directly above and below this "hole" such that a complex network of hydrogen bonding interactions is established between the template, the framework and the bridging hydroxyl groups (see Figure 5b).

The role of hydrogen bonding in controlling the precise layer topology is particularly well illustrated in compounds **3** and **4** and the related mineral zippiete.[56] All three materials have very similar layer topologies consisting of uranium pentagonal bipyramids surrounded by five molybdenum tetrahedra (see Figure 5). Two distinct Mo^{VI} tetrahedra are observed, A which contains one terminal and three bridging oxygen atoms and B which contains two bridging and two terminal oxygen atoms. The molybdenum tetrahedra are labeled A and B in Figure 6a and b, with each uranium polyhedron is corner linked to three tetrahedra of type A and two of type B. However, the manner in which these tetrahedra surround the uranium polyhedra differs. As seen in Figure 5a, in **3** the three A tetrahedra are on one side of the uranium polyhedra, with the B tetrahedra on the opposite side, thus producing an AAABB sequence. Whereas in **4** the three A tetrahedra are separated by a B tetrahedron, resulting in a AABAB sequence (see Figure 5b). The layer topology observed in **4** is identical to that of zippiete,[56] which has a molybdenum tetrahedral sequence of AABAB (see Figure 6c). The small structural differences in each layer are attributable to the orientation of the terminal Mo−O bonds. In zippiete each terminal Mo−O bond is directed toward the potassium cations, whereas in **3** and **4** the terminal oxygen atoms are directed into the layers such that the hydrogen bonding interactions between the template and the terminal oxygen atoms are maximized.

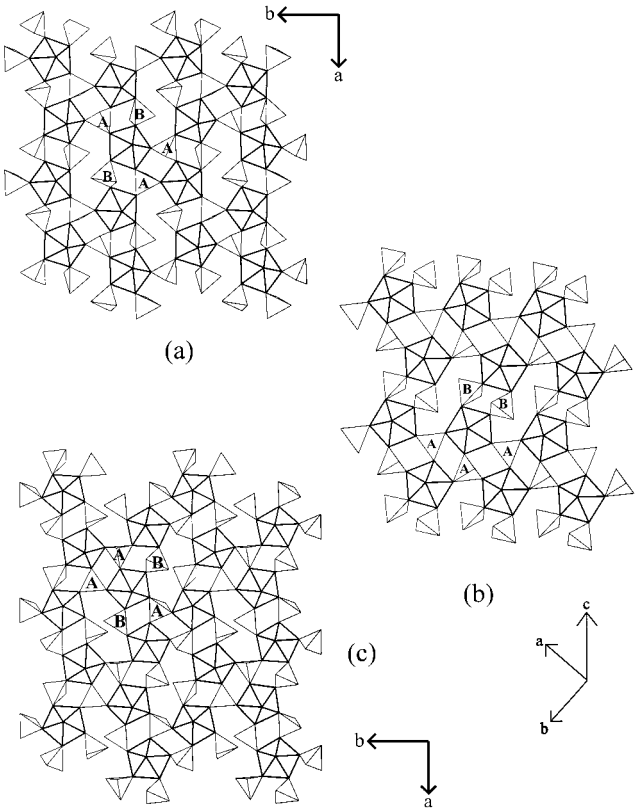

Figure 6. Polyhedral representation of the uranium molybdate layer in (a) $(C_4H_{12}N_2)(UO_2)(MoO_4)_2$, (b) $(C_5H_{14}N_2)(UO_2)(MoO_4)_2 \cdot H_2O$, and (c) zippiete, $K_2[UO_2(MoO_4)_2]$.

Conclusion

We have reported the phase pure syntheses, structures, and spectroscopy of the first examples of organically templated uranium molybdates. The isolation of compounds **1**−**4** is a further example of the utility of template mediated hydrothermal synthesis for the synthesis of a range of diverse structure types in which the organic template is incorporated into the inorganic framework. The range of topologies exhibited in compounds **1**−**4** reflects the profound influence of the organic template in directing the formation of a particular topology. Although the synthesis of a microporous uranium based material remains an ongoing challenge, the structural diversity of phases **1**−**4** and the existence of a large number of uranium molybdate mineral phases suggests that with the correct choice of templating species and reaction conditions the synthesis of further novel phases, including three-dimensional microporous materials, is a realizable goal.

Acknowledgment. The authors thank BNFL, EPSRC, and the Leverhulme Trust (R.J.F.) for support. P.S.H. thanks Christ Church, University of Oxford, for a Junior Research Fellowship.

(58) Serezhkin, V. N.; Trunov, V. K.; Makarevich, L. G. *Kristallografiya* **1980**, *25*, 858.
(59) Burns, P. C.; Miller, M. L.; Ewing, R. C. *Can. Miner.* **1996**, *34*, 845.

Supporting Information Available: The powder XRD pattern of the calcined material and four X-ray crystallographic files, in CIF format, are available free of charge via the Internet at http://pubs.acs.org.

IC980836R